

## Original paper

## Open Access

R.Tesser\*, R. Vitiello, G. Carotenuto, C. Garcia Sancho, A.Vergara, P.J. Maireles Torres, Changzhu Li, M. Di Serio

# Niobia supported on silica as a catalyst for Biodiesel production from waste oil

**Abstract:** The activity and stability of niobia supported on silica catalyst have been tested in continuous micro-pilot reactors, for biodiesel production starting from acid vegetable oils. A catalyst was prepared by the impregnation of silica pellets with a loading of 12% of Nb and was extensively characterized. The activity of this catalyst in both esterification and transesterification was tested in a continuous micro-pilot laboratory plant in which acid oil was fed (FFA 10% w/w) at a temperature of 220°C and at a pressure of 60 bar. The niobia based catalyst resulted in a very active catalyst in both esterification (FFA conversion = 95-90%) and transesterification reactions (FAME yield = 80-90%), and the activity remained quite constant for more than 100 h on stream. Notwithstanding this stability, a non-negligible leaching phenomena has been detected, in the case of long-time continuous runs, as the Nb concentration on the spent catalyst resulted lower than that on the fresh one. The obtained result confirms that the leaching of the active specie is one of the most strong problem in heterogeneous catalysis for biodiesel production.

**Keywords:** niobia supported catalyst, acid catalysis, esterification, transesterification

DOI 10.1515/cse-2015-0002

Received March 11, 2015; accepted March 20, 2015

\*Corresponding author: R.Tesser: University of Naples "Federico II", Faculty of Science MM.FF.NN., Department of Chemical Science, E-mail: riccardo.tesser@unina.it

R. Vitiello, G. Carotenuto, A.Vergara, M. Di Serio: University of Naples "Federico II", Faculty of Science MM.FF.NN., Department of Chemical Science.

R.Tesser, R. Vitiello, M. Di Serio: CIRCC, Italy.

C. Garcia Sancho, P.J. Maireles Torres: University of Málaga, Faculty of Sciences, Department of Inorganic Chemistry, Crystallography and Mineralogy.

Changzhu Li: Hunan Academy of Forestry.

## 1 Introduction

The decrease of the availability of crude oil and consequently its increasing price, as well as the environmental concerns, has attracted the interest towards the production of biofuels. Biodiesel, a mixture of fatty acid alkyl esters, usually methyl esters (FAME), is the second largest produced biofuel after bioethanol, and 22 Mton were produced worldwide [1]. Nowadays, the main route to obtain biodiesel is the transesterification of triglycerides (mainly vegetable oils, such as rapeseed, palm and soybean oils) with methanol, using homogenous alkaline metal hydroxides or methoxides (KOH, NaOH, NaOCH<sub>3</sub>, KOCH<sub>3</sub>) at low temperature (50-80°C) [2-3]. The coproduced glycerol is separated from FAME through settling. One of the main drawbacks in biodiesel production is the price of raw materials (usually, refined vegetable oils), corresponding to about 80% of the final product cost [3]. Moreover, biodiesel production from refined vegetable oil is in competition with food production.

The use of waste oils and non-edible oils can solve the previous cited problems, being the objective of second-generation biofuels. The share of biodiesel produced from waste/non edible oils in global biodiesel production is expected to increase by 10% per year in next 10 years [1]. However, this choice imposes to modify the technology of biodiesel production [2]. As a matter of fact, the suggested raw materials are characterized by a high content of free fatty acids (FFA >> 1% w/w), which will produce soaps with the classical basic homogeneous catalysts. The formation of soaps poisons the catalyst and, in mean time, prevents the separation of biodiesel from glycerol due to the formation of stable emulsions.

One of the most reliable ways to treat raw materials containing high concentration of FFA, is the use of an acid catalyst which can promote both the esterification of FFA and transesterification of triglycerides [4].

In this sense, homogenous Brønsted acid catalysts (such as sulphuric, sulfonics, phosphoric and hydrochloric acids) [5] and Lewis acid catalysts [4,6,7]

have been proposed to catalyze both the esterification and transesterification reactions in biodiesel production, but their use foresees high costs of the process due to the plant maintenance and/or product purification and/or waste catalyst disposal. Heterogeneous acid catalysts represents a great challenge that could allow this to overcome the above mentioned drawbacks [8,9]. It must be pointed out that Brønsted acid catalysts are mainly active in promoting esterification reaction, while Lewis acid catalysts are more active in transesterification [10]. Therefore, both acid sites of suitable strength should be present on the surface of an ideal heterogeneous catalyst [10].

Moreover, it must be taken considered a possible deactivation of catalysts, which could be due to (i) the leaching of active phase (ii) the fouling of the surface or (iii) the poisoning of the active sites. Consequently, the development of suitable regeneration methods is a key point in the search of very active solid acid catalysts to be used in a new technology for biodiesel production [11].

Several heterogeneous acid catalysts have been proposed in the recent literature for biodiesel production: mixed metal oxides, sulphonated resins, sulphated metal oxides, heteropolyacids, vanadyl phosphate and many others [10,12].

In particular, niobium-based materials, previously employed as useful acid catalysts for many catalytic reactions [13,14], have also yielded promising results in biodiesel production. Thus, Portilho *et al.*, for example, claimed the use of niobic acid treated with a phosphoric acid solution and niobium oxide supported on alumina as efficient catalysts for the transesterification of canola oil with methanol or ethanol [15]. García-Sancho, *et al.*, showed that biodiesel can be produced via methanolysis of sunflower oil in the presence of a MCM-41 silica containing niobium oxide [16]. This mesoporous niobosilicate can be used even in the presence of oleic acid (2.2 wt%) and water (0.4 wt%), without losing activity [16]. On the other hand, niobic acid (hydrated niobium oxide,  $\text{Nb}_2\text{O}_5 \cdot n\text{H}_2\text{O}$ ) has already been proposed as catalyst for the esterification of FFA with methanol or ethanol [17,18]. Niobia supported on silica [19] and on silica-alumina [20] has been used as catalysts for the esterification of acetic acid with alcohols. Niobium–silicon mixed oxide nanocomposites, prepared by a sol–gel method, showed the presence of active sites for transesterification of triglycerides and esterification of FFA [21].

In the present paper, the performance of niobia supported by impregnation on silica in biodiesel production from soybean oil containing a high FFA concentration (a waste oil model), has been deeply investigated. The catalytic behavior has also been

determined in a continuous tubular reactor in order to evaluate the suitability of this catalyst for the development of an industrial process.

## 2 Methods

### 2.1 Catalysts synthesis

The supported  $\text{Nb}_2\text{O}_5$  catalysts with different loading concentrations (3–12%  $\text{Nb}_2\text{O}_5$ ) were prepared by dry impregnation of niobium oxalate [22], obtained from niobium pentoxide [23], on a commercial silica (Engelhard). The commercial silica sample is of spherical shape (mean diameter = 3–5 mm). The catalysts have been prepared by impregnation of both the pellets and of the powder obtained by grinding in a mortar the commercial silica (powder diameter < 100  $\mu\text{m}$ ). After impregnation, the catalysts were dried at 60°C for 10 h and calcined at 900°C for 6 h. The denominations of all the catalysts used in the catalytic tests with their compositions are reported in **Table 1**.

### 2.2 Catalysts characterization

Textural analyses were carried out by using a Thermoquest Sorptomatic 1990 Instrument (Fisons Instrument) by determining the nitrogen adsorption-desorption isotherms at 77 K. The samples were thermally pre-treated under vacuum overnight up to 473 K (heating rate = 1 K/min). Specific surface area ( $S_{\text{BET}}$ ) were determined by using the BET method.

Powder X-ray diffraction (XRD) patterns were obtained using a Philips powder diffractometer. The scans were collected in the range 5–80° (2 $\theta$ ) using Cu K $\alpha$  radiation with a rate of 0.01° (2 $\theta$ /s). The X-ray tube operated at 40 kV and 25 mA.

X-ray photoelectron (XPS) studies were performed with a Physical Electronics PHI 5700 spectrometer equipped

**Table 1:** Niobia content and surface area of the catalysts and the support (xNbSi, powder; 12NbSi(l), pellets)

| Support/Catalyst                   | wt % $\text{Nb}_2\text{O}_5$ | Surf. Area ( $\text{m}^2/\text{g}$ ) |
|------------------------------------|------------------------------|--------------------------------------|
| $\text{SiO}_2$                     | -                            | 291                                  |
| $\text{SiO}_2$ (calcined at 900°C) | -                            | 285                                  |
| 3NbSi                              | 3                            | -                                    |
| 5NbSi                              | 5                            | -                                    |
| 12NbSi                             | 12                           | 266                                  |
| 12NbSi(l)                          | 12                           | 250                                  |

with a hemispherical electron analyzer (model 80-365B) and a Mg  $K_{\alpha}$  (1253.6 eV) X-ray source. High resolution spectra were recorded at 45° take-off-angle in the constant pass energy mode at 29.35 eV. Charge referencing was done against adventitious carbon (C1s at 284.8 eV). The pressure in the analysis chamber was kept lower than  $5 \times 10^{-6}$  Pa. A PHI ACCESS ESCA-V6.0 F software package was used for acquisition and data analysis. A Shirley-type background was subtracted from the signals. All recorded spectra were always fitted using Gaussian-Lorentzian curves to more accurately determine the binding energy of the different element core levels.

Confocal Raman microscope (Jasco, NRS-3100) was used to obtain Raman spectra. The 647-nm line of a water cooled Kr+ laser (Coherent), 800 mW, was injected into an integrated Olympus microscope and focused to a spot size of approximately 2  $\mu\text{m}$  by a 100x objective. A holographic notch filter was used to reject the excitation laser line. Raman scattering was collected by a peltier-cooled 1024  $\times$  128 pixel CCD photon detector (Andor DU401BVI). For most systems, it takes 60 s to collect a complete data set.

The surface acidity of the 12NbSi catalyst was evaluated by Temperature Programmed Desorption of  $\text{NH}_3$  ( $\text{NH}_3$ -TPD), which has been conducted using the *Thermo Finnigan TPD/R/O 1100*. Before the  $\text{NH}_3$ -TPD measurement, the powdered catalyst (0.1–0.2 g) was outgassed in a flow of pure helium (20  $\text{cm}^3/\text{min}$ ), at different treatment temperature (600, 300 and 50 °C) for 30 min. Then, the sample was cooled at 40°C and saturated with a stream of 10%  $\text{NH}_3$  in He (20  $\text{cm}^3/\text{min}$ ) for about 30 min. Afterward, the catalyst was purged in a helium flow until a constant baseline was attained. The ammonia desorption was determined in the temperature range of 40–500 °C with a linear heating rate of 10 °C  $\text{min}^{-1}$  in a flow of He (10  $\text{cm}^3/\text{min}$ ). Desorbed  $\text{NH}_3$  was detected by a Thermal Conductivity Detector (TCD). The eventual presence of water in the evolving gases was removed by a trap containing anhydrous magnesium perchlorate, located between the detector and the reactor.

The measurement of acid strength of the 12NbSi catalyst was also done by the Hammett indicators (Neutral red,  $\text{p}K_{\text{a}} = 6.8$ ; Butter yellow,  $\text{p}K_{\text{a}} = 3.3$ ; Benzeneazodiphenylamine,  $\text{p}K_{\text{a}} = 1.5$ ; Dicinnamalacetone,  $\text{p}K_{\text{a}} = -3$ ; Benzalacetophenone,  $\text{p}K_{\text{a}} = -5.6$ ). The measurements were done on samples freshly dried at 300°C before carrying out the indicator tests, and handled in a dry box. Moreover, the tests were also performed on the sample after contacting with the air for 72 h, with the aim to verify the effect of the humidity adsorption on the surface acidity.

The acidity of the 12NbSi catalyst was also investigated by using pyridine adsorption, coupled to FTIR spectroscopy. The spectra were recorded on a Shimadzu Fourier Transform Infrared Instrument (FTIR8300). Selfsupported wafers were placed in a vacuum cell, with greaseless stopcocks and  $\text{CaF}_2$  windows.

Before pyridine adsorption, the 12NbSi sample was thermally treated at 300°C in air for 2 h, followed by evacuation at  $10^{-2}$  Pa for 2h at the same temperature. Following this pretreatment, the wafer was cooled to room temperature and a spectrum was recorded as reference. In a second set of experiments, the pretreatment was excluded to verify the effect of the dehydration on the surface acidity.

### 2.3 Catalytic tests

The screening of the catalysts was performed using a series of 5–6 small stainless steel vial reactors. The reactants, soybean oil or acid soybean oil (FFA =10%, w/w) (2 g) and methanol (0.88 g), and a defined amount of the catalyst (0.1 g) were introduced in each reactor. The reactors were introduced in a ventilated oven which initial temperature was fixed at 50°C for 14 min, and then increased at a rate of 20°C/min until it reached the reaction temperature, 180°C, which was kept for 1 h. At the end, the reactors were quenched in a cold bath. Blank runs (without catalyst) were also performed to evaluate any contribution of the non-catalytic reaction.

The most active catalyst was also tested under the same experimental conditions used by García-Sancho et al. [16] with a MCM-41 silica containing niobium oxide (methanol/sunflower oil molar ratio= 12, Cat= 5 wt%,  $T=200^\circ\text{C}$ ,  $t= 4$  h).

One of the most interesting aspects concerning the use of heterogeneous catalysts is the absence of soluble homogeneous species in the reaction medium [24]. After catalyst filtration, the concentration of niobium in solution was determined by using the UV-visible standard procedure [25] with the purpose to measure the eventual leaching.

On the other hand, to achieve information on the catalyst life in the industrial reaction conditions, some runs have been performed at 220 °C in a laboratory continuous micropilot plant using the best catalytic system. The reaction system consisted of a stainless steel packed bed reactor of 30 cm of length and  $d=1/2$  inch. A weighted amount of the 12NbSi catalyst, as pellets (12NbSi(I), 30 g), was charged in the reactor. The measured void fraction was 0.66. The reaction was carried out at constant pressure of 60 bars by using a back-pressure regulator.

Two different runs were performed: using silica pellets (reference test, run 0) and with 12NbSi (I) catalyst pellets (run 1).

The soybean oil or the acid soybean oil (FFA = 10%) flow rate was fixed at 2.6 ml/min while for methanol 5.3 ml/min was used. Samples of the outlet reaction mixture were withdrawn at different times on stream. The FAME (fatty acid methyl esters) yields were determined by using the HNMR technique (Bruker 200 MHz) measuring the area of the  $H^1_{NMR}$  signal related to methoxylic and methylenic groups using the following equation [26]:

$$Y_{FAME} = 100 \frac{A_{1/3}}{A_{2/3}}$$

where (A1) and (A2) are the area of H-NMR signal related to methoxylic and methylenic groups, respectively.

FFA concentration is determined by measuring the residual FFA concentration by titration ( $w_{FFA}$ ) [27].

The free fatty acid (FFA) conversion ( $IFFA$ ) was calculated using the following equation:

$$\lambda_{FFA} = \frac{w_{FFA}^0 - w_{FFA}}{w_{FFA}^0} 100$$

The conversion of glyceride groups ( $IGly$ ) (due to the transesterification reaction) can be calculated using the following equation [4]:

$$\lambda_{Gly} = Y_{FAME} \left( 1 + \frac{PM_{oil}}{3PM_{OA}} \frac{w_{FFA}^0}{100 - w_{FFA}^0} \right) - \lambda_{FFA} \frac{PM_{oil}}{3PM_{OA}} \frac{w_{FFA}^0}{100 - w_{FFA}^0}$$

Were:

$PM_{oil}$  = molecular weight of soybean oil, [g/mol]

$PM_{OA}$  = molecular weight of oleic acid, [g/mol]

$w_{FFA}$  = initial FFA concentration, [% w/w]

The stability of the catalyst was verified by determining, after 100 h on stream, the content of niobium on the discharged catalyst was determined by ICP-MS (Inductively Coupled Plasma Mass Spectrometry).

## 3 Results and Discussion

### 3.1 Preliminary Catalytic Screening

First of all, since at high temperatures the stainless steel internal surface of the vials could catalyze the transesterification and esterification reactions, different runs without catalyst were performed at 180 °C using acid oil as reagent, obtaining FAME yields in the range 7-10% and a FFA conversion of 15-20%.

The influence of the amount of niobia on the catalytic activity has been studied and the obtained results are reported in Figure 1.

As it can be seen, by increasing the amount of supported niobia a significant increment of the FFA conversion was obtained. Calcined silica exhibits a very low activity (the obtained conversion is in the range of the blank runs). However, the activity improves significantly (35% of FFA conversion) in the case of 3NbSi, which

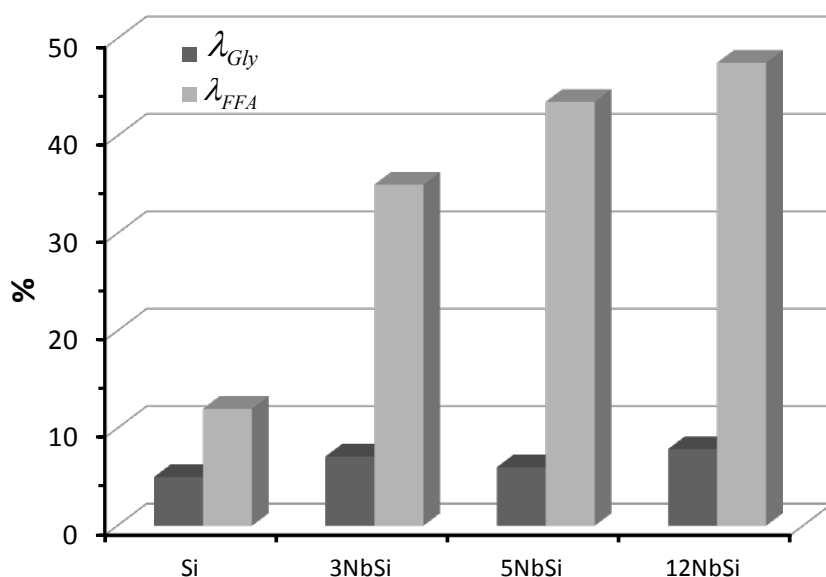


**Figure 1:** The conversion of triglycerides ( $IGly$ ) and FFA ( $IFFA$ ) of acid soybean oil (FFA =10% w/w) obtained with  $Nb_2O_5$  supported on silica catalysts. Reaction time = 1 h, reaction temperature = 180°C, catalyst = 0.1 g, acid soybean oil = 2 g, methanol =0.88 g.

possesses the lowest  $\text{Nb}_2\text{O}_5$  loading (3%). A further increase of the amount of supported niobium oxide does not lead to an important amelioration of the catalytic activity, with FFA conversions of 42% and 48% for 5NbSi (5%  $\text{Nb}_2\text{O}_5$ ) and 12NbSi (12%  $\text{Nb}_2\text{O}_5$ ), respectively.

On the other hand, the transesterification activity (glyceride group conversion) is relatively low and it is minimally affected by the niobia loading, under these experimental conditions.

The leaching tests were carried out for each catalyst, confirming the stability of this family of supported niobia catalysts, since the presence of Nb in the filtered solution was not evidenced by UV-Vis analysis.

The best catalyst (12NbSi) was also tested in the same condition used by García-Sancho et al. with a MCM-41 silica containing niobia (methanol/sunflower oil molar ratio= 12, Cat= 5 wt%, T=200°C, t= 4h) [16]. The obtained result (70% FAME yield) was lower than that obtained with a niobia supported on a MCM-41 silica catalyst with a 8%  $\text{Nb}_2\text{O}_5$  (87% FAME yield). However, the cost of the MCM-41 silica synthesis is higher than that of a commercial silica and, for an industrial application, the use of the latter type of silica as support is favored (if the catalyst stability is proven also for a long reaction time). Moreover, the catalytic results pointed out that the 12NbSi catalyst has good activity also in transesterification reaction when the temperature is increased until 200°C. This is in agreement with data reported by García-Sancho et al. [16], who found an important amelioration of the transesterification activity, by using the MCM-41 silica containing niobia, increasing the temperature from 175°C to 200°C.

## 3.2 Catalyst Characterizations

The textural characteristics of the most active catalyst (12NbSi) were determined from the  $\text{N}_2$  adsorption-desorption isotherms at -196°C. The adsorption of niobia on silica has little effect on the specific surface area (see Tab. 1) and no crystalline phases could be determined by XRD, even for the catalyst with the highest niobia loading, 12NbSi (see Fig.2), in agreement with the literature data [28,29].

This fact reveals that niobium is well dispersed on the silica surface.

Xray photoelectron spectroscopy has been used to get insights into the surface nature of catalysts. The XPS data are summarized in Table 2. The Si 2p signal is symmetrical and appears at binding energy (BE) values of 103.2–103.8 eV, typical of Si in silica. The O 1s region only shows a single and almost symmetric peak at BE: 532.6–533.5 eV, close to the value observed for a silica (533.1 eV), whereas bulk  $\text{Nb}_2\text{O}_5$  displays this peak at lower BE (530.2 eV), thus corroborating the absence of segregated  $\text{Nb}_2\text{O}_5$  particles on the external surface of the siliceous support, as can be also deduced from the highest surface Si/Nb molar ratio in comparison with the corresponding bulk values (Table 2). On the other hand, the two components of the Nb 3d doublet appear at 206.3–206.9 eV ( $3d_{5/2}$ ) and 208.8–209.6 eV ( $3d_{3/2}$ ) when commercial silica is used as support, whereas this doublet is observed at higher BE in the case of MCM-41-based materials. However, in both cases, these BE values have been reported for Nb(V) in an oxidic environment. On the other hand, the surface Si/Nb atomic ratio values

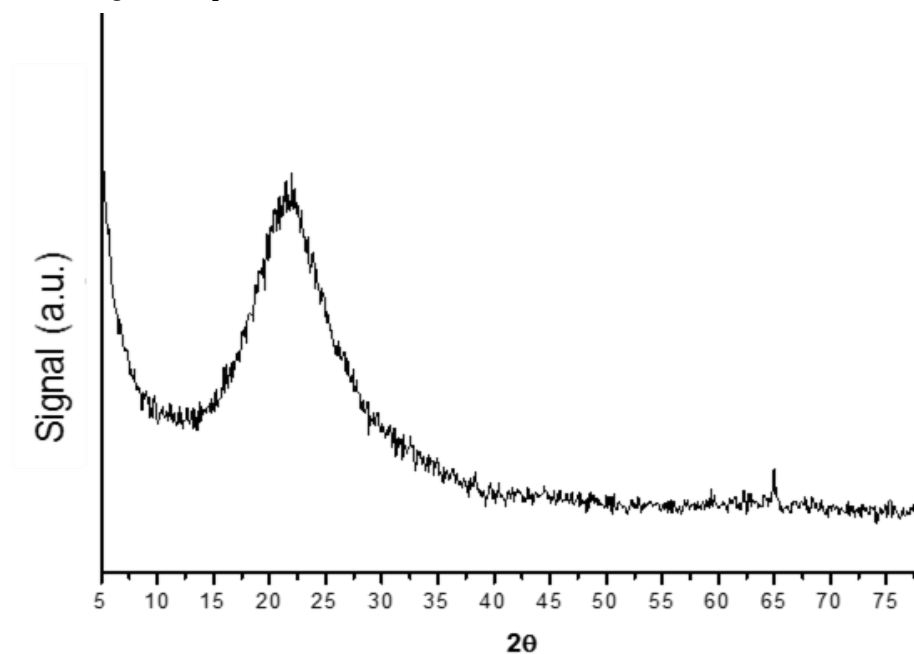


Figure 2: Powder XRD pattern of the 12NbSi catalyst.

**Table 2.** XPS data (binding energies and Si/Nb atomic ratios) of catalysts.

| Catalyst         | Si 2p (eV) | O 1s (eV) | Nb 3d (eV)   | Surface Si/Nb atomic ratio | Bulk Si/Nb atomic ratio |
|------------------|------------|-----------|--|----------------------------|-------------------------|
| 5NbSi_rt         | 103.8      | 533.2     | 206.4 (3d <sub>5/2</sub> )<br>209.0 (3d <sub>3/2</sub> ) | 271                        | 42.1                    |
| 12NbSi_rt        | 103.8      | 533.2     | 206.3<br>208.8   | 48.9                       | 16.3                    |
| 12NbSi_300       | 104.1      | 533.5     | 206.4<br>209.0   | 183.5                      | 16.3                    |
| 12NbSi_300_spent | 103.3      | 532.7     | 206.9<br>209.6   | 267                        | 16.3                    |
| MCM-Nb8_rt       | 103.6      | 533.0     | 208.0<br>210.6   | 51.2                       | 22.7                    |
| MCM-Nb8_spent    | 103.2      | 532.7     | 207.7<br>210.4   | 73.4                       | 22.7                    |

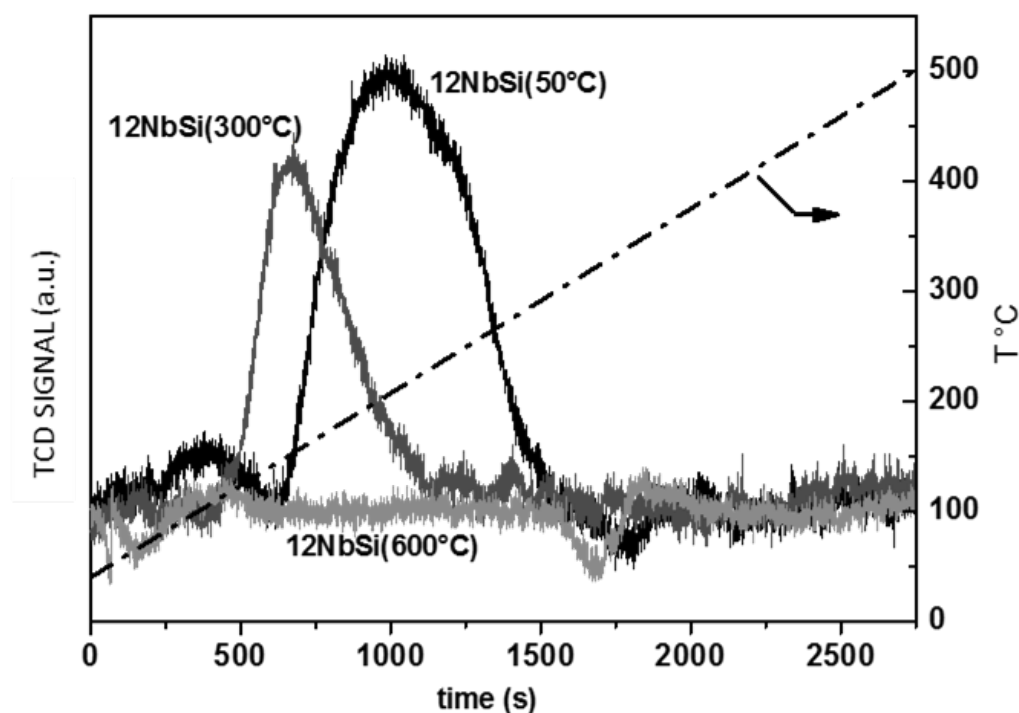
are higher than the corresponding bulk ones (Table 2), which is a consequence of the presence of niobia into the pores, thus difficult to detect by this XPS technique. After reaction, these ratio increases due to the covering of the active sites by organic species, as can be inferred from the surface carbon analysis, which yields values as high as 43 and 61% for the spent 12NbSi and MCM-8Nb, respectively.

The surface acidity of the 12NbSi catalyst has been evaluated by temperature programmed desorption of adsorbed NH<sub>3</sub> (see Fig. 3). Before NH<sub>3</sub> adsorption, the catalyst was pretreated at 600°C. Surprisingly, the 12NbSi catalyst didn't show any desorption peak. This data are

in contrast with the highest esterification activity found with this 12NbSi catalyst. For this reason, the TPD analysis was repeated after pre-treating at lower temperature (300°C and 50°C) (see Fig. 3), and acid sites were now detected, decreasing with the increase of the pretreatment temperature.

Shirai *et al.* found for a niobia/silica catalyst that, after pretreatment at high temperature, the Brønsted acid sites disappeared, while the Lewis acid sites are independent from the pretreatment temperature [19].

This fact has been confirmed by FTIR analysis of adsorbed pyridine (Fig. 4). The 12NbSi catalyst, pretreated

**Figure 3:** NH<sub>3</sub>-TPD profiles for the 12NbSi catalyst pretreated at 600°C, 300°C and 50°C.

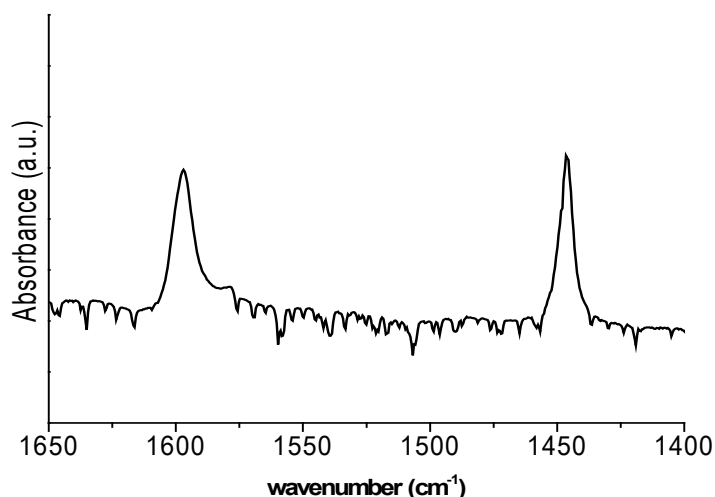


**Figure 4:** FTIR spectrum of adsorbed pyridine of the 12NbSi catalyst (pretreated at 300°C overnight under vacuum) at 25°C.

at 300°C overnight under vacuum, only showed at 25°C the vibration modes associated to pyridine adsorbed on Lewis acid sites at 1445  $\text{cm}^{-1}$  and 1600–1610  $\text{cm}^{-1}$  [19,28,30]. However, the acid sites are very weak, since these bands were not observed after evacuation at 150°C.

However, the formation of stronger acid sites after exposure to the air moisture has been confirmed by the use of Hammett indicators. The 12NbSi catalyst, previously dried at 300°C and handled in a dry box, didn't show any acidity. When the catalyst was put at ambient condition, after 2 h, the acid strength was determined with Hammett indicator ( $-5.6 < \text{p}K_{\text{a}} < -3$ ).

In order to elucidate the structure-activity relationships, Raman spectroscopy has been used to characterize the 12NbSi catalyst, and the spectra were collected at ambient condition and wet (sample was wet and then the spectrum was registered without dehydration), and were compared with that of  $\text{Nb}_2\text{O}_5$  as reference (Fig. 5).

It has been reported that regular tetrahedral  $\text{NbO}_4$  structures are associated to Raman frequencies appearing in the 790–830  $\text{cm}^{-1}$  region, distorted  $\text{NbO}_6$  octahedra in the 500–700  $\text{cm}^{-1}$  region and highly distorted octahedral  $\text{NbO}_6$  structures give rise to bands in the 850–1000  $\text{cm}^{-1}$  region [31]. A Raman feature at 995  $\text{cm}^{-1}$  and 938–934  $\text{cm}^{-1}$ , observed in the spectra of 12NbSi and wet 12NbSi, can be related to the symmetric stretching vibration modes associated to terminal mono-oxo Nb = O bonds of  $\text{NbO}_6$  octahedra belonging to the H- $\text{Nb}_2\text{O}_5$  structure [32–35]. By comparison with the  $\text{Nb}_2\text{O}_5$ , the signal at 995  $\text{cm}^{-1}$  should correspond to the bulk  $\text{Nb}_2\text{O}_5$  species [36]. On the other hand, the vibration bands around 630  $\text{cm}^{-1}$  can be associated with polymerized surface

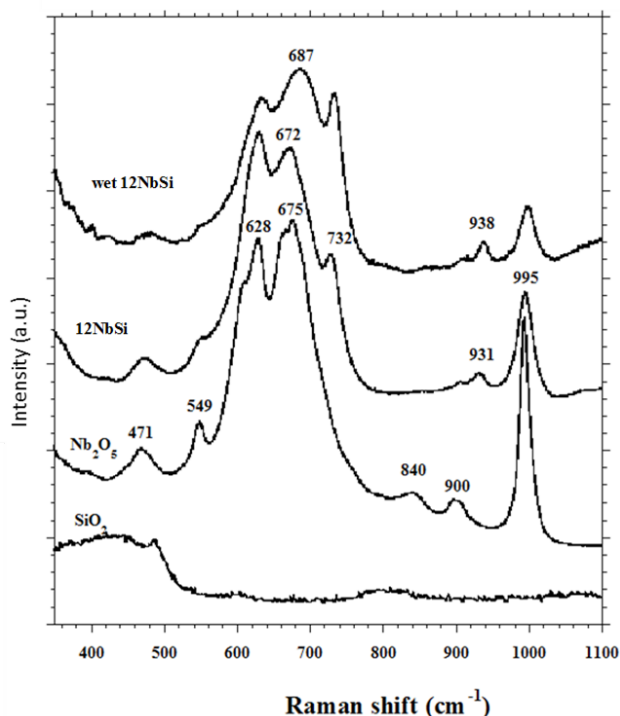


**Figure 5.** Raman spectra of the 12NbSi catalyst, at ambient condition and wet (wet12NbSi),  $\text{Nb}_2\text{O}_5$  and  $\text{SiO}_2$ .

metal oxide species (M-O-M and -O-M-O- vibrations) [36]. Ultimately, the Raman technique confirms the presence of small  $\text{Nb}_2\text{O}_5$  particles, not detected by XRD, on samples with high niobium content on silica [37].

Although the Raman spectra of 12NbSi and wet 12NbSi are similar, they aren't identical as evidence the different relative intensities of the Raman signals at 995  $\text{cm}^{-1}$  and 730  $\text{cm}^{-1}$ .

The characteristic bands at  $995\text{ cm}^{-1}$  and  $940\text{ cm}^{-1}$  of  $\text{Nb=O}$  species that are associated to Lewis acid sites [37] are still present on the wet 12NbSi catalyst; however, the formation of more Nb-OH groups cannot be excluded because the change of spectra in the region of distorted octahedral  $\text{NbO}_6$  structures ( $500\text{-}700\text{ cm}^{-1}$ ).

The previous data confirm the well established observation that the molecular structure of niobia supported on silica is influenced by the hydration degree [35,37].

On the other hand, when the niobia/silica catalyst is immersed in aqueous solution, Brönsted acid sites are predominantly generated by coordination of the water molecules to Lewis acid sites [28].

### 3.3 Effect of pretreatment on catalytic activity

As it has been previously mentioned, pretreatment conditions affect greatly on the catalyst acidity. In order to evaluate its influence on the catalytic activity, different runs have been done with the catalyst dried at  $300^\circ\text{C}$  and handled in a dry box, and the catalyst remained in contact with atmosphere for 2 h (Fig.6).

The dry 12NbSi catalyst exhibits a high activity in the transesterification reaction ( $I_{\text{GLY}} = 48\%$ ) and a low activity in the esterification reaction ( $I_{\text{FFA}} = 20\%$ ), whereas the behavior of the wet sample is inverse: the activity in the esterification process ( $I_{\text{FFA}} = 50\%$ ) is higher than that of the transesterification reaction ( $I_{\text{GLY}} = 5\%$ ), and they are similar to that reported in Fig. 1 for the 12NbSi catalyst.

These results agree well with those derived from the characterization and data previously reported on the relative activity of Lewis and Brönsted acid sites [10,38,39]: the Lewis acid sites present on dried catalysts favor the transesterification reaction while the esterification process is more favored by Brönsted acid sites, formed after exposure to the atmosphere.

### 3.4 Continuous runs

Using the silica pellets (30 g) as catalyst (run 0) (Methanol  $5.6\text{ cm}^3/\text{min}$ ; acid oil  $2.6\text{ cm}^3/\text{min}$  (FFA =  $9.5\%$  w/w),  $T=220^\circ\text{C}$ ), a conversion of 20-30% of FFA was obtained with a total FAME yield of 25-30 %.

The results obtained with pellets of the 12 NbSi catalyst, under similar experimental conditions (run 1), are reported in Fig. 7.

The results are very interesting since this 12NbSi catalyst was very active in both esterification (FFA conversion = 95-90%) and transesterification reactions (FAME yield = 80-90%), and the activity remained constant for more than 100 h on stream.

However, in order to verify the stability of the catalyst, the niobium content on discharged catalyst was determined by ICP-MS. Unfortunately, a leaching phenomena was discovered, because the niobia content in the spent catalyst was 3%-5% instead of 12%.

Nevertheless, this niobia content in the catalyst is enough active (see data reported in Fig. 1) and, from the conversion data in the continuous run, the leaching cannot be inferred (probably the conversions are near the equilibrium values).

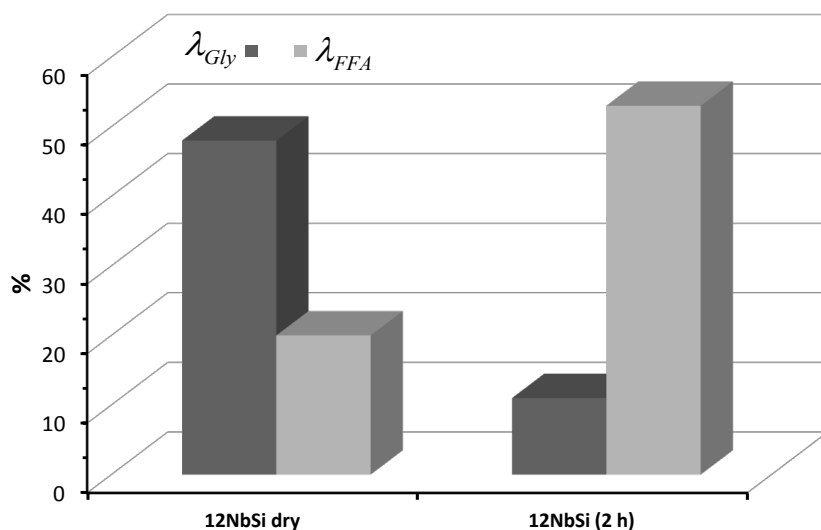


**Figure 6:** The conversion of glyceride groups ( $I_{\text{GLY}}$ ) and of FFA ( $I_{\text{FFA}}$ ) of acid soybean oil (FFA =  $10\%$  w/w) obtained with the 12NbSi catalyst. 12NbSi dry = dried at  $300^\circ\text{C}$ ; 12NbSi (2 h) = exposed to atmosphere for 2 h; (Reaction time = 1 h, reaction temperature =  $180^\circ\text{C}$ , catalyst = 0.1 g, acid soybean oil = 2 g, methanol = 0.88 g)

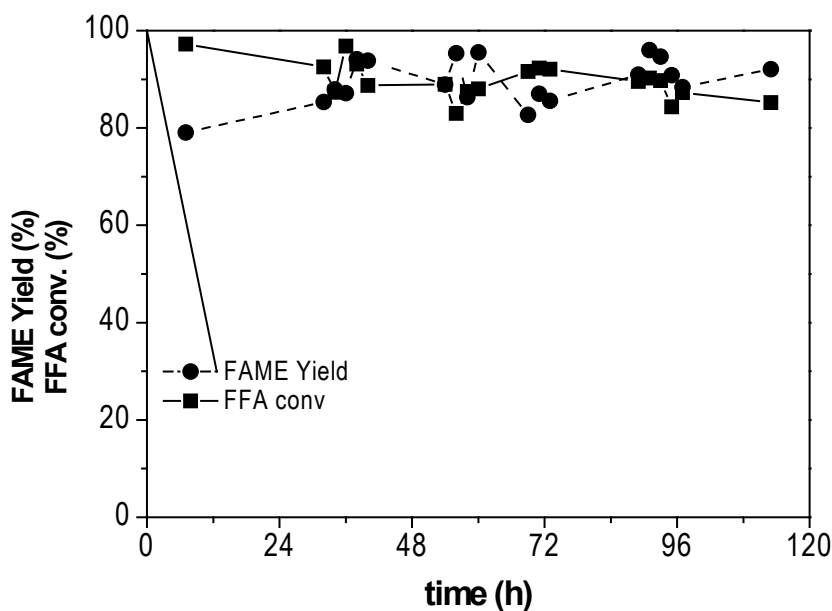


**Figure 7-** FFA conversion and FAME yield obtained in continuous run 1. Methanol 5.3 cm<sup>3</sup>/min; acid oil 2.6 cm<sup>3</sup>/min (FFA = 10 % w/w); T=220°C; Cat. 12NbSi.

The obtained results confirm that the leaching is one of the most strong problem in heterogeneous catalysis for biodiesel production [24].

## 4 Conclusions

The distribution of strength and nature of acid sites on niobia supported on silica is strongly dependent on the environment in contact with the catalyst. When the catalyst is dried, Lewis acid sites are mainly present, whereas the contact with atmosphere favors the reaction with the humidity and the formation of Brønsted acid sites of moderate strength ( $-5.6 < \text{pK}_a \leq -3$ ).

Niobia supported on silica is active in both esterification of FFA and transesterification of triglycerides, with no loss of activity in the continuous run for 100 h. However, the characterization of the used catalyst revealed the slow leaching of niobia, which reduces its potential of industrial application in biodiesel production, if this problem will be not solved.

## References

- [1] OECD/FAO “Biofuels”, in OECD-FAO Agricultural Outlook 2012, OECD Publishing, 2012 [http://dx.doi.org/10.1787/agr\\_outlook-2012-6-en](http://dx.doi.org/10.1787/agr_outlook-2012-6-en).
- [2] Ma F., Hanna M.A., *Bioresour. Technol.* 70 (1999) 1-15
- [3] Gerpen J. Van, *Fuel Process. Technol.* 86 (2005) 1097 – 1107
- [4] Di Serio M., Tesser R., Dimiccoli M., Cammarota F., Nastasi M., Santacesaria E., *J. Mol. Cat. A:Chem* 1-2 (2005) 111-115.
- [5] Zhang Y., Dubè M., McLean D., Kates M., *Bioresour. Technol.* , 89 (2003), 1.
- [6] Abreu F. R., Lima D.G., Hamú E.H., Einloft S., Rubim J. C., P.A.Z. Suarez, *J. Am. Oil Chem. Soc.* 80 (2003) 601-604
- [7] Di Serio M., Carotenuto G., Cucciolo M.E., Lega M., Ruffo F., Tesser R., Trifuoggi M., *J. Mol. Cat. A:Chem* 353– 354 (2011) 106 – 110
- [8] Lotero E., Goodwin J.G., Bruce D.A., Suwannakarn K., Liu Y., Lopez D.E., *Catalysis* 19 (2006) 41-84
- [9] Kulkarni M.G., Dalai A., *Ind. Eng. Chem. Res.* , 45 (2006) 2901-2913.
- [10] Di Serio M., Tesser R., Peng Mei L., Santacesaria E., *Energy & Fuels* 22 (2007) 207-217
- [11] Di Serio M., Mallardo S., Carotenuto G., Tesser R., Santacesaria E., *Cat. Today* 195 (2012) 54–58
- [12] Melero J., Iglesias J., Morales G., *Green Chem.* 11 (2009) 1285-1308
- [13] Tanabe K., Okazaki S., *App. Catal. A*, 133 (1995) 191–218
- [14] Ziolk M., *Cat. Today* 78 (2003) 47-64
- [15] Portilho M., Vieira J., Zotin J., Lima M., M. (2008) US Pat. 0295393 A1
- [16] García-Sancho C., Moreno-Tost R., Mérida-Robles J.M., Santamaría-González J., Jiménez-López A., Maireles-Torres P., *App. Cat. B: Env.* 108-109 (2011) 161– 167
- [17] Aranda D.A.G., Antunes O.A., PCT No. WO 2006/081644 (2006).
- [18] De Araújo Gonçalves J., Ramos A. L. D., Rocha L.L.L., Domingos A.K., Monteiro R.S., Peres J.S., Furtado N.C., Taft C.A., Aranda D.A.G., *J. Phys. Org. Chem.* 24 (2011) 54–64

- [19] Shirai M., Asakura K., Iwasawa Y., *J. Phys. Chem* 95 (1991) 9999-10004
- [20] Braga V.S., Barros I.C.L., Garcia F.A.C., Dias S.C.L., Dias J.A., *Cat. Today* 133–135 (2008) 106–112
- [21] Di Serio M., Turco R., Pernice P., Aronne A., Sannino F., Santacesaria E., *Cat. Today*, 192 (2012) 112-116
- [22] Jehng J.M., Wachs I.E., *J. Phys. Chem.* 95 (1991) 7373-7379
- [23] Medeiros F., Moura F., da Silva F., Souza C., Gomes K., Gomes U., Brazilian U.; *J. Chem. Eng.* 23 (2006) 531-538.
- [24] Di Serio M., Tesser R., Casale L., Trifuoggi M., Santacesaria E., *Top. Catal.* 53 (2010) 811-819
- [25] Snell F., Ettore L., *Encyclopedia of industrial chemical analysis*, Interscience, New York, 1974
- [26] Gelbard G., Brès O., Vargas R.M., Vielfaure F., Schuchardt U.F., *J. Am. Oil Chem. Soc.* 72 (1995) 1239-1241
- [27] ASTM D803-82 (colourimetric method)
- [28] Denofre S., Gushiken Y., de Castro S.C., Kawano Y., *J. Chem. Faraday Trans.* 89 (1993) 1057-1061
- [29] Carniti P., Gervasini A., Marzo M., *J. Phys. Chem.* 112 (2008) 14064-14074
- [30] Lahousse C., Aboulayt A., Mauge F., Bachelier J., Lavalley J., *J. Mol. Catal.* 84 (1993) 283-297
- [31] Yoshida S., Nishimura Y., Tanaka T., Kanai H., Funabiki T., *Cat. Today*, 8 (1990) 67–75
- [32] McConnell A.A., Anderson J.S., Rao C.N.R., *Spectrochim Acta*, 32 (1976) 1067-1076
- [33] Jehng J.M., Wachs I.E., *Chem. Mater.* 3 (1991) 100-107
- [34] Wachs I.E., *Cat. Today* 27 (1996) 437-455.
- [35] Pittman R., Bell A., *J. Phys. Chem.* 97 (1993) 12178-12185.
- [36] Vuurman M.A., Wachs I.E., *J. Phys. Chem.*, 96 (1992) 5008-5016
- [37] Jehng J.M., Wachs I.E., *Cat. Today*, 8 (1990) 37-55
- [38] Shi W., Zhao J., Yuan X., Wang S., Wang X., Huo M., *Chem. Eng. Technol.* 35 (2012) 347–352
- [39] Aronne A., Turco M., Bagnasco G., Ramis G., Santacesaria E., Di Serio M., Marenga E., Bevilacqua M., Cammarano C., Fanelli E., *Applied Catalysis A: General*, 347, 2,(2008), 179-185